Available online at www.sciencedirect.com
ScienceDirect
Applied Catalysis B: Environmental 79 (2008) 63–71
APPLIED CATALYSIS B: ENVIRONMENTAL
www.elsevier.com/locate/apcatb

Photocatalytic discoloration of Methyl Orange on innovative parylene–TiO_2 flexible thin films under simulated sunlight

Yu Zhiyong [a,e], H. Keppner [b], D. Laub [c], E. Mielczarski [d], J. Mielczarski [d], L. Kiwi-Minsker [a], A. Renken [a], J. Kiwi [a,*]

[a] *Institute of Chemical Sciences and Engineering, LGRC, Station 6, EPFL, 1015 Lausanne, Switzerland*
[b] *University of Applied Sciences, 7 Av de l'Hotel de Ville, CH-2400 Le-Locle, Switzerland*
[c] *Interdepartamental Institute of Electron Microscopy (CIME), Station 12, EPFL, 1015 Lausanne, Switzerland*
[d] *INPL/CNRS, UMR 7569 LEM, 15 Av du Charmois, 54501 Vandoeuvre les Nancy, France*
[e] *Department of Chemistry, Renmin University of China, 100872 Beijing, China*

Received 20 February 2006; received in revised form 28 September 2007; accepted 1 October 2007
Available online 11 October 2007

Abstract

Parylene films loaded with TiO_2 are reported as photocatalysts in azo dye discoloration processes. The TiO_2 loading of the parylene film was 0.32% (w/w) and the amount of TiO_2 on the film was about two orders of magnitude below the TiO_2 added in suspension to discolore the same solution of Methyl Orange used as a probe. The parylene/TiO_2 films showed a similar activity in the presence of O_2 or H_2O_2 during the discoloration of dyes. This shows the efficient role of O_2 as e_{cb}^- scavenger. The photonic efficiency of the parylene/TiO_2 film during the Methyl Orange discoloration was 0.04. Based on X-ray photoelectron spectroscopy (XPS) data, the TiO_2 particles loaded on the parylene film were shown to be at first encapsulated in the polymer. After the encapsulation is broken, the TiO_2 particles are fully exposed to the dye solution. The lack of surface intermediates like C-residues, N and S-species after the photocatalytic process implies an efficient decomposition of the dye at the catalyst interface. During the dye degradation carbonates and carboxylates were detected by XPS and Fourier transform infrared spectroscopy (FTIR) disappearing at the end of the discoloration process. Evidence is presented during the photocatalysis for the formation of a composite parylene/TiO_2 film. The formation of this composite involves surface modification of parylene (partial lost of chlorine) in the outermost surface layer with concomitant densification of the TiO_2 particles on the parylene film. The parylene film presented a side with high rugosity and one with low rugosity attaching different amounts of TiO_2 in each case as observed by transmission electron microscopy (TEM).

Keywords: Parylene films; Discoloration of azo dye; Photocatalysis; TEM; IR; XPS

1. Introduction

In the field of environmental chemistry, semiconductor mediated photocatalysis has been the focus of recent attention since it aims at the destruction of contaminants in water and air in non-toxic processes and low operational temperature. These low cost processes can also use sunlight as the source of irradiation [1–4]. Suspensions of TiO_2 as photocatalysts present two major obstacles when used in the form of suspension: (a) the separation of TiO_2 after the treatment and (b) the low quantum efficiency of these processes. Suitable supports for TiO_2 in the form of glass plates, Raschig rings, films and fabrics have been reported recently by our group on Nafion [5], glass mats [6], polyethylene–maleic anhydride copolymer [7], inorganic C-fabrics [8], synthetic fabrics [9], natural fabrics [10] and Tedlar, a commercial fluorocarbon film [11]. Suitable supports should present four properties: (a) withstand reactive oxidative radicals attack during light, (b) maintain adequate long-term catalytic stability, (c) preclude TiO_2 leaching during the light irradiation, (d) allow photocatalytic reaction to proceed with an acceptable kinetics.

In this study we report for the first time the use of parylene thin films as a support for TiO_2 in processes activated by simulated solar irradiation. We will present the details of the TiO_2 loading procedure. The use of XPS spectroscopy will give detailed information on the surface composition of the

* Corresponding author.
E-mail address: John.Kiwi@epfl.ch (J. Kiwi).

0926-3373/$ – see front matter © 2007 Elsevier B.V. All rights reserved.
doi:10.1016/j.apcatb.2007.10.006

outermost catalyst layer (at a few nm) during the dye photodiscoloration process with very high sensitivity. The signals obtained reveal the significant changes taking place at the parylene/TiO_2 surface after different reaction times of dye decomposition.

Commercial applications of parylene thin films relate to their protective function on plastic surfaces and take advantage of its biocompatible nature. Parylene thin films are used on mobile telephone and other plastic gadgets used in medical applications [1–3] hindering the attack by chemical and/or corrosive agents due to the stable nature and chemical inertness of these films. High density parylene-C film can be heated up to 180 °C and its stability is comparable to the one reported for polyethylene. This study will show that parylene/TiO_2 films show a stable performance during the photoinduced discoloration of Methyl Orange intervening with an acceptable kinetics during the dye discoloration. The parylene/TiO_2 films require a much lower TiO_2 concentration per unit volume than the TiO_2 suspensions to photodegrade azo dyes. The parylene/TiO_2 film avoids the screening of the incident light by the TiO_2 particles in suspension. Studies involving the abatement of azo dyes in suspensions of TiO_2 have been previously reported [1,2,4,12,13].

2. Experimental

2.1. Materials

Reagents like acid and bases, dye material and H_2O_2 were p.a. from Fluka AG Buchs, Switzerland, and used without further purification. Millipore-Q tri-distilled H_2O was used throughout this study. The photocatalyst TiO_2 Degussa P25 powder was a gift from Degussa AG. Parylene (di-*para*-dichloro-xylylene) thin films (45 μm thick) were obtained from the University of Applied Sciences, Section Microtechnologies, La Locle, CH-2400, Switzerland. The scheme of preparation of the parylene-C polymer is shown in Fig. 1. Parylene-C has the highest density compared to other types of parylene A and B not shown in Fig. 1.

The functional formula of parylene-C is shown in the left hand-side of Fig. 1. The chemical formula of the repetitive unit in this fluor-polymer is commonly noted as –CH_2CHFCH_2CHF–. The film remains tough, flexible and fatigue-resistant up to 180 °C (flowing point) for long operational periods.

2.2. Catalyst preparation

A 10 g/l TiO_2 Degussa P25 suspension was added to 200 ml isopropanol and aged for a day. The parylene-C film was then introduced in this suspension for 10 h and the film was dried afterwards in air at room temperature (23 °C). The dried film was then heated in an oven at 180 °C for 6 h. Finally the parylene/TiO_2 film was sonicated for 25 min and washed with tri-distilled water four consecutive times to eliminate the loosely bound TiO_2 particles from the film surface.

2.3. Irradiation procedures and analyses of the irradiated solutions

The photodegradation of Methyl Orange was carried out in small batch cylindrical photochemical reactors made from Pyrex glass (cutoff λ = 290 nm) of 70 ml capacity containing 50 ml aqueous solution. The strips 48 cm^2 films of parylene/TiO_2 were positioned immediately behind the reactor wall. Irradiation of the samples was carried out in the cavity of a Suntest solar simulator (Hanau, Germany) air cooled at 45 °C. The light intensity in the cavity of the Suntest simulator at tuned at 100 mW/cm^2 (AM 1) was 2×10^{16} photons/s cm^2. The Suntest Xe-lamp emitted 7% of the photons in the 290–400 spectral range. The integral radiant flux in the reactor cavity was monitored with a power-meter from YSI Corp., CO, USA. The absorption of the solutions was followed in a Hewlett-Packard 38620 N-diode array spectrophotometer. The disappearance of

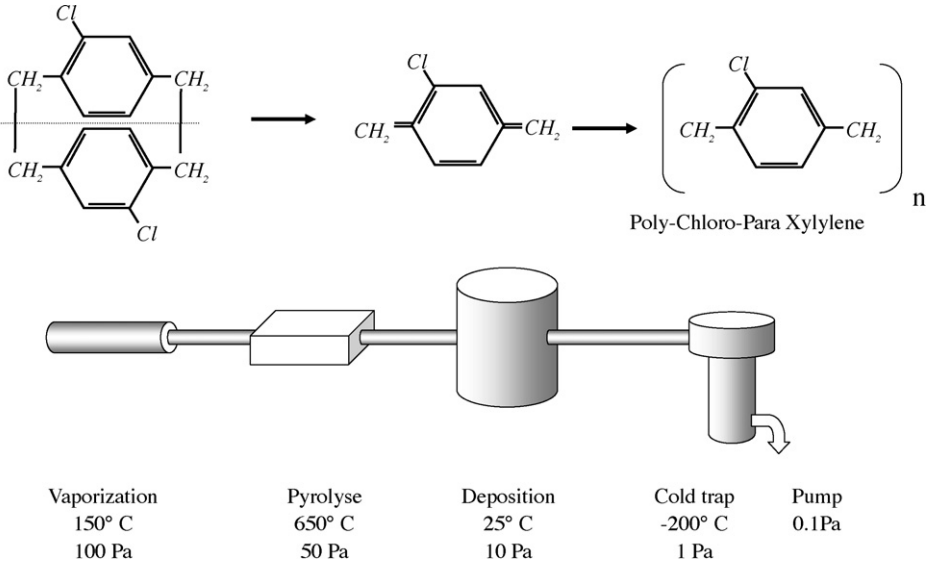

Fig. 1. Schematic of the fabrication process of the parylene thin film.

Methyl Orange was measured in the spectrophotometer at $\lambda = 465$ nm (the absorption peak). The peroxide concentration of the solutions were measured using Merckoquant® paper from Merck AG, Switzerland. This was carried out for reactions with initially added H_2O_2 to determine its concentration in the course of the reaction.

2.4. Transmission electron microscopy (TEM) of parylene/TiO_2 films

A field emission TEM microscope Philips EM 430 (300 kV) was used to measure the particle size of the titania aggregates on the parylene-C surface. Energy dispersive X-ray spectroscopy (EDS) was used to identify the deposition of TiO_2 on the parylene-C film. The parylene film was coated with EPON 812 epoxy resin polymerized at 60 °C and then cut with a microtome at room temperature to a thin layer of ~50 nm thickness. Magnification of 10,000 up to 450,000× were used to characterize the samples. The resolution normally used was of 0.5 nm.

2.5. Elemental analysis

Elemental analysis of the TiO_2 coverage on parylene-C was carried out by atomic absorption spectrometry using a Perkin-Elmer 300S unit.

2.6. X-ray photoelectron spectroscopy (XPS)

The XPS was performed using Mg Kα radiation of 150 W. The electron energy analyzer (Leybold EA200) was operated at a band-pass energy of 75 eV in the pre-selected transmission mode. The binding energy of the spectrometer was referenced to 84.0 eV for the Au $4f_{7/2}$ signal according to the SCA A83 standard of the National Physics Laboratory. The evaluation of the binding energies of the embedded Fe-clusters was carried out following the standard procedures [14,15]. A reproducibility of ±5% was attained in the XPS measurements. The ADS100 set was utilized to evaluate the XPS data by subtraction of X-ray satellites applying the background correction according to Shirley [14]. The presence of electrostatic charging effects was controlled by measurements including charge compensation by changing the electrostatic potential at the aperture site of the electron energy analyzer.

2.7. Fourier transform infrared spectroscopy

The detailed description of the applied internal reflection FTIR technique and procedure used have been previously reported [16]. The infrared reflection spectra of the catalyst samples were recorded on a Bruker IFS55 FTIR spectrometer equipped with an MCT detector and a reflection ATR attachment. A ZnSe reflection element (47 × 20 × 3) with incident angle 45° was used in these studies. These accessories were from Harrick Scientific Co. The unit of intensity was defined as $-\log(R/R_o)$, where R_o and R are the reflectivities of the reflectivity element and with the Nafion membranes, respectively. Both sample and reference spectra were averaged over the same number of 1000 scans.

2.8. X-ray diffraction measurements (XRD) of parylene/TiO_2

The crystallinity and phase of the TiO_2 loaded on parylene-C was studied with a Siemens X-ray diffractometer using Cu Kα radiation as the power source.

3. Results and discussion

3.1. Discoloration of Methyl Orange photocatalyzed by parylene/TiO_2 under simulated solar light irradiation. Effect of light intensity

Fig. 2A presents the runs showing the photodiscoloration of dilute solutions of Methyl Orange under Suntest simulated solar light irradiation. Control experiments in the dark in the presence of the paryelne-C film alone (trace a) or in the presence of parylene/TiO_2 (trace b) or under Suntest light irradiation in the presence of parylene (trace c) were practically not conducive to Methyl Orange discoloration. But under light irradiation in the presence of the photocatalyst parylene/TiO_2 (trace d) the dye photodiscoloration was observed within 6 h. The interaction between Methyl Orange and TiO_2 is favored at the biocompatible pH used (5.9) by the positive charge of $TiOH_2^+$ existing on the TiO_2 Degussa P25 (IEP 7.0) [17] interacting by electrostatic attraction with the anion radical of Methyl Orange at pH 5.9 after the Na-cation ionizes in aqueous solution [18]. The photodegradation of Methyl Orange on parylene/TiO_2 films was also carried out at different pH values. In the acid range the dye degradation proceeded within times well below the time of 6 h shown in Fig. 2A (trace d). This is due to the stronger electrostatic attraction between the Methyl Orange radical anion and the charged positively charged TiO_2 ($TiOH_2^+$). At pH values >7, the TiO_2 is in the form of TiO^- and therefore the electrostatic interaction with the Methyl Orange radical anion is not favored at basic pH values leading to degradation times >6 h.

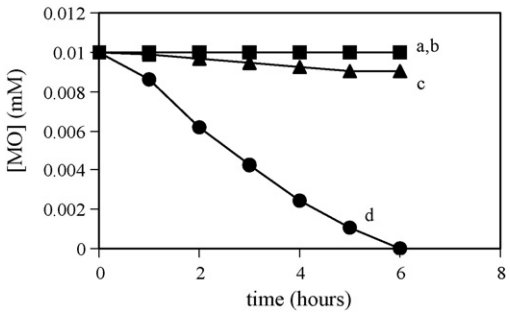

Fig. 2A. Discoloration and photodiscoloration of Methyl Orange (0.01 mM) in a solution containing Parylene or Parylene/TiO_2 film at initial pH = 5.9. (a) dark reaction in the presence of Parylene, (b) dark reaction in the presence of Parylene/TiO_2 film, (c) reaction under Suntest solar simulated light (90 mW/cm^2) in the presence of Parylene film, (d) reaction under Suntest solar simulated light (90 mW/cm^2) in the presence of Parylene/TiO_2 film.

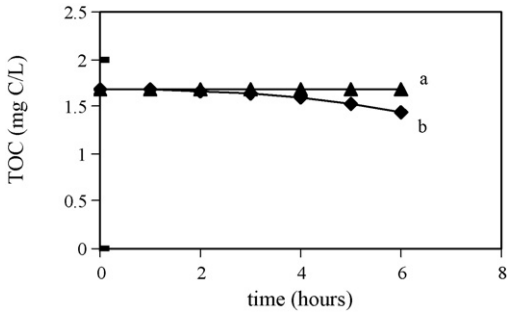

Fig. 2B. TOC reduction of Methyl Orange (0.01 mM) at initial pH = 5.9. Other experimental conditions like in Fig. 2a. (a) homogeneous solution of the dye under Suntest light irradiation, (b) in the presence of Parylene/TiO_2 film under Suntest light irradiation.

Fig. 2B shows the TOC data when the Methyl Orange solution is irradiated in the absence of parylene/TiO_2 (Fig. 2B, trace a) or in the presence of parylene/TiO_2 (Fig. 2B, trace b). Only a modest reduction of 17% in the TOC value was observed in the presence of the photocatalyst.

Fig. 3 shows the repetitive photodegradation of Methyl Orange during four consecutive cycles. After each cycle, the parylene/TiO_2 is washed thoroughly with water and a fresh solution of Methyl Orange is added before each photocatalytic run in the photoreactor. The results observed show a similar degradation kinetics for the consecutive runs in Fig. 3. This points out to the stable performance of the parylene/TiO_2 film conserving its initial photoactivity.

Fig. 4 (traces a and b) shows the photodiscoloration of Methyl Orange in homogeneous solution under two simulated solar light intensities. Practically no photodegradation of Methyl Orange occurs in both cases. In the presence of the parylene/TiO_2 film, the photodiscoloration takes place as shown in traces (c and d). The favorable effect of the light intensity is seen when the applied light intensity is increased from 60 to 90 mW/cm^2. This implies that the saturation of Methyl Orange acting as a photosensitizer has not been reached. As long as the degradation becomes more efficient when the intensity of the applied light is increased, no saturation of the Methyl Orange is reached in solution within the range of the applied intensities.

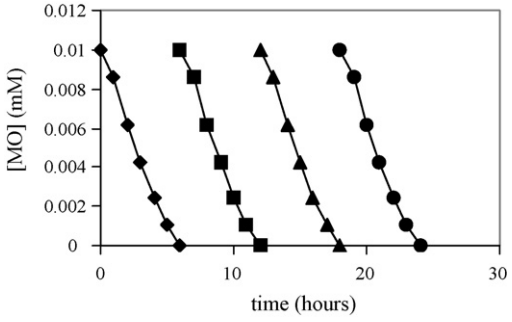

Fig. 3. Repetitive photodiscoloration cycles of Methyl Orange (0.01 mM) under Suntest solar simulated light (90 mw/cm^2) in the presence of Parylene/TiO_2. Initial pH = 5.9.

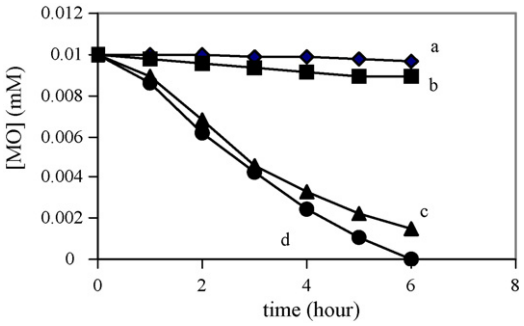

Fig. 4. Effect of the light intensity on the photodiscoloration of Methyl Orange (0.01 mM) at initial pH = 5.9. (a) photolysis of the solution with Suntest solar simulated light (60 mW/cm^2), (b) photolysis of the solution with Suntest solar simulated light (90 mW/cm^2), (c) photolysis of the solution with Suntest solar simulated light (60 mW/cm^2) in the presence of Parylene/TiO_2 film, (d) photolysis of the solution with Suntest solar simulated light (90 mW/cm^2) in the presence of Parylene/TiO_2 film.

Solutions of Methyl Orange II of 0.01, 0.02 and 0.04 mM were irradiated under Suntest simulated light tuned at 90 mW/cm^2. The photodiscoloration rates observed followed pseudo-first order kinetics and the observed rates decreased as the concentration of Methyl Orange in the solution was increased.

The mechanism of azo dyes mediated by TiO_2 under light irradiation in the presence of O_2 as oxidant has been reported [12,19–21]. The dye molecules are excited by the light photons and produce the singlet excited state as reported by Vinodgopal and Kamat [19] and by Bandara and Kiwi [20] for azo dyes

$$(\text{Methyl Orange})_{ads} + h\nu \rightarrow {}^1(\text{Methyl Orange})_{ads}{}^* \quad (1)$$

An electron is injected from the excited state of the adsorbed Methyl Orange in the conduction band of TiO_2 leading to the Methyl Orange cation that subsequently decays:

$$ {}^1(\text{Methyl Orange})_{ads}{}^* + TiO_2 \rightarrow {}^1(\text{Methyl Orange})_{ads}{}^{\bullet+} + TiO_2\,(e^-) \quad (2)$$

and the $e_{cb}{}^-$ is subsequently scavenged by the O_2 adsorbed on the TiO_2 surface generating the superoxide radical $O_2{}^{\bullet-}$ [1–4]

$$TiO_2\,(e^-) + O_2 \rightarrow TiO_2 + O_2{}^{\bullet-} \quad (3)$$

At the biocompatible pH worked in Figs. 1–3 the formation of $HO_2{}^{\bullet}$ and H_2O_2 takes place

$$O_2{}^{\bullet-} + H^+ \rightarrow HO_2{}^{\bullet} \quad (4)$$

$$HO_2{}^{\bullet} + O_2{}^{\bullet-} + H^+ \rightarrow H_2O_2 + O_2 \quad (5)$$

$$HO_2{}^{\bullet} + H^+ + TiO_2\,(e^-) \rightarrow H_2O_2 + TiO_2 \quad (6)$$

Nevertheless, the concentrations of H_2O_2 found in solution were observed to remain a relatively low level of ~0.5 mg/l, but the O_2 present in the solution was sufficient to enhance the charge separation at the TiO_2 surface allowing reactions (3)–(6) to proceed. There is also a fraction of the H_2O_2 adsorbed on the

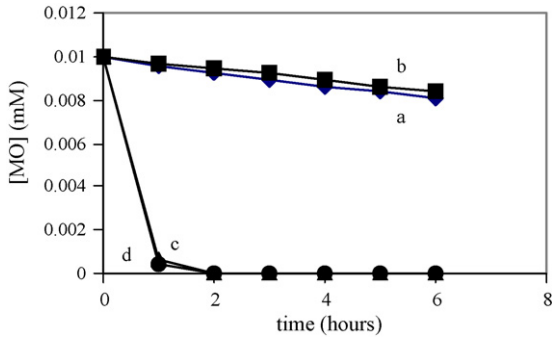

Fig. 5. Discoloration and photodiscoloration of Methyl Orange (0.01 mM) in a solution containing TiO_2 Degussa P-25 (0.5 g/L) suspension at initial pH = 5.9. (a) dark reaction, (b) dark reaction in the presence of H_2O_2 (1 mM), (c) reaction with Suntest solar simulated light (90 mW/cm^2) in the presence of a TiO_2 suspension only, (d) reaction with Suntest solar simulated light (90 mW/cm^2) in the presence of a suspension of TiO_2 and H_2O_2 (1 mM).

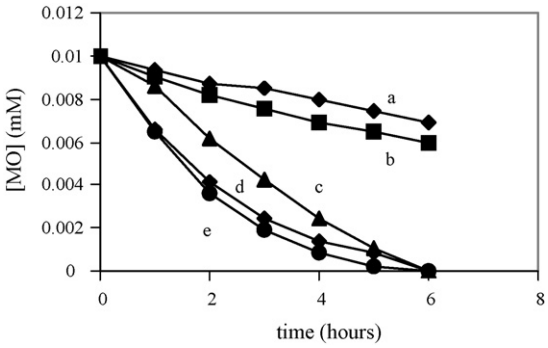

Fig. 6. Effect of H_2O_2 concentration on the photodiscoloration of Methyl Orange (0.01 mM) with Suntest solar simulated light (90 mw/cm^2). (a) in the presence of H_2O_2 (1.0 mM), initial pH = 5.8, (b) in the presence of H_2O_2 (2.0 mM), initial pH = 5.6, (c) in the presence of Parylene/TiO_2 film but no H_2O_2 added, initial pH = 5.9, (d) in the presence of Parylene/TiO_2 film and H_2O_2 (1.0 mM), initial pH = 5.8, (e) in the presence of Parylene/TiO_2 film and H_2O_2 (2.0 mM), initial pH = 5.6.

TiO_2 surface available for oxidative reactions as reported elsewhere [22].

3.2. Effect of the H_2O_2 on the dye discoloration

Fig. 5 shows the discoloration and photodiscoloration of Methyl Orange mediated by TiO_2 Degussa P25 powders (0.5 g/l). It can be seen that the discoloration of Methyl Orange by TiO_2 (trace a) is very slow. In the presence of H_2O_2 (1 mM), the discoloration in the dark of Methyl Orange (trace b) is also very slow. But under Suntest solar simulated radiation the Methyl Orange photodiscoloration due to the TiO_2 suspension (trace c) and with added H_2O_2 (1 mM) (trace d) is fast. Fig. 5 (traces c and d) shows that the Methyl Orange solution is discolored in 1 h. The relative photonic efficiency is the ratio of dye disappearance to the incident photon flux on the reactor cell walls in a defined time period. This number allows the standardization of photochemical processes when using different experimental conditions in different laboratories.

$$\text{Photonic efficiency} = \frac{\text{molecules of dye reacted}}{\text{light quanta reaching the reactor wall}} \quad (7)$$

In Fig. 5 (trace c and d) taking the Suntest light flux as 1.6 photons/s cm^2, the volume in the reactor as ~50 ml and the cell wall surface of 48.8 cm^2, the photobleaching of Methyl Orange (0.01 mM) would proceed with a photonic efficiency of ~0.04 within 1 h.

Fig. 6 (traces a and b) presents the effect of the concentration of H_2O_2 on the degradation of Methyl Orange in homogeneous solution. Fig. 6 (trace c) shows the effect of the parylene/TiO_2 film on the photodiscoloration of Methyl Orange and Fig. 6 (traces d and e) show the favorable effect of the increase of the H_2O_2 concentration on the photodiscoloration. The electron acceptor role of H_2O_2 enhancing the charge separation at the TiO_2 surface is noted in Eq. (8)

$$H_2O_2 + TiO_2\,(e_{cb}^-) \rightarrow OH^- + OH^\bullet + TiO_2 \quad (8)$$

3.3. Transmission electron microscopy of TiO_2 particles on parylene-C films

Fig. 7 presents the TEM of parylene-C film obtained from a microtome slice of 50 nm. Since the parylene-C film is grown on the flat glass surface in the reactor, the side sticking on the glass plate presents a very low rugosity compared to the side of the film exposed to the gas atmosphere inside the preparative reactor. This high rugosity side shows a much higher amount of TiO_2 as it will be shown by transmission electron microscopy below. Fig. 8a presents the TiO_2 Degussa P25 coverage on the low rugosity side of the parylene-C film at time zero having a media width of 150 μm. This corresponds to about 5 layers of TiO_2 with a crystal size of ~30 nm. Fig. 8b presents the TiO_2 Degussa P25 particle coverage of the high rugosity side with an average width comprising 30–40 layers of TiO_2. Fig. 9a shows the TEM of the low rugosity side after 6 h photodiscoloration of

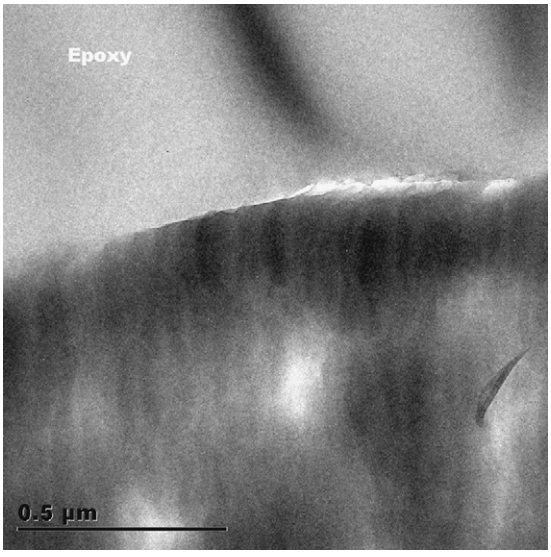

Fig. 7. Transmission electron microscopy (TEM) epoxy coated parylene-C film. The folding in the dark area of the epoxy region is due to the microtome cut introduced during the sample preparation.

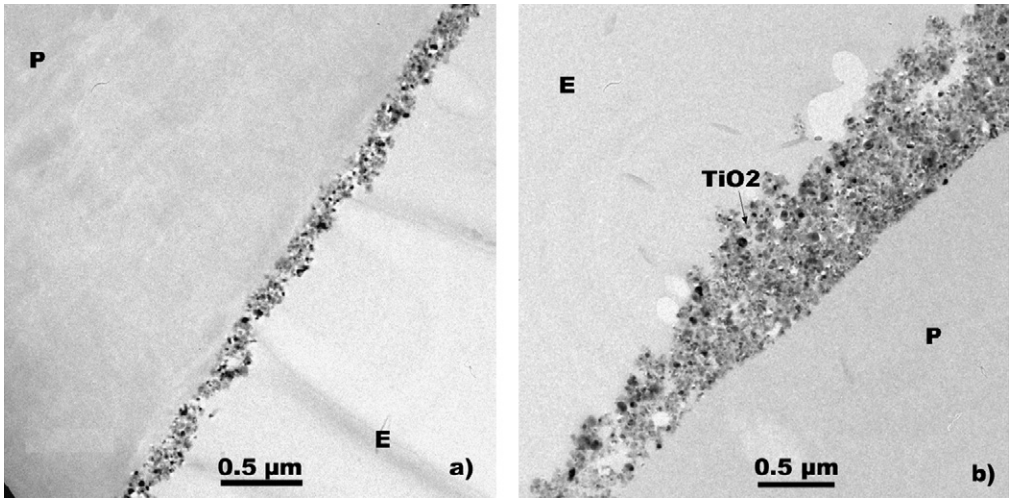

Fig. 8. TEM of parylene/TiO_2 at time zero before the photodiscoloration of Methyl Orange: (a) the TiO_2 Degussa P25 particles on the low rugosity side of the parylene-C film. The term P refers to parylene and E to the epoxide layer and (b) the TiO_2 Degussa P25 particles on the high rugosity side of the parylene-C film.

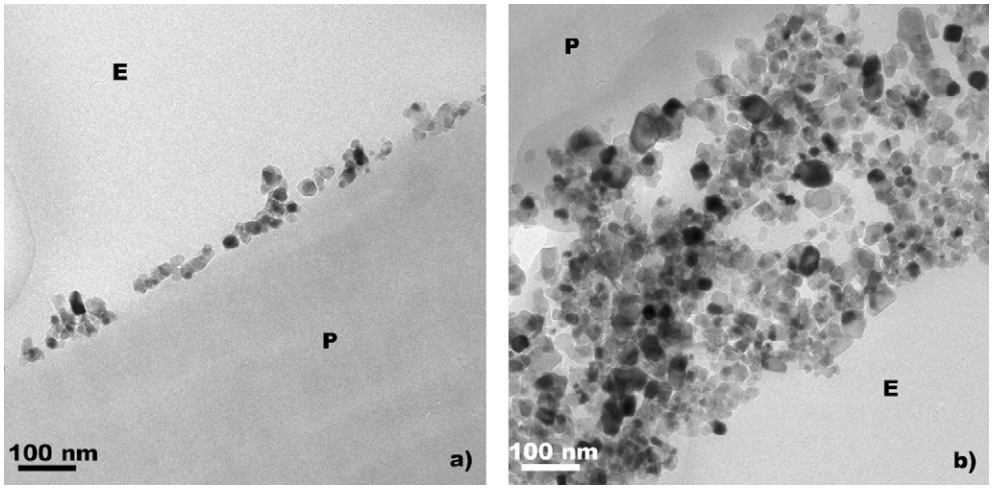

Fig. 9. TEM of parylene/TiO_2 after 6 h photodiscoloration of Methyl Orange: (a) low rugosity side of the parylene-C film with TiO_2 Degussa P25 particles. The term P refers to parylene and E to the epoxide layer. (b) High rugosity side of the parylene-C film with TiO_2 Degussa P25.

Methyl Orange (Fig. 2A, trace d). A thin irregular layer of TiO_2 (∼60 nm) comprising two layers on the average is observed. The high rugosity side (Fig. 9b) presents the same width for the TiO_2 layers of the parylene/TiO_2 film after the photocatalytic process as found at time zero. This parylene-C thin film was used over several months in the photodiscoloration conserving the surface morphology reported in Fig. 9b. Since the repetitive photodiscoloration of Methyl Orange reported in Fig. 3 proceeds with the same kinetics, it can be suggested that the loss of TiO_2 from the low rugosity side is compensated by an increase in light penetration reaching the rougher side in the photocatalyst. This seems the reason for a stable catalyst performance observed for the parylene/TiO_2 during long-term operation. The TiO_2 loading of the parylene-C film was 0.32% (w/w) before use and 0.31% (w/w) after use. The small decrease observed in the final overall TiO_2 loading can be explained by the fact that from the outset the low rugosity side had a very low TiO_2 loading. Its decrease was not significant in the overall composition of the photocatalyst. The parylene/TiO_2 film used had a surface of 48 cm^2 and a loading of 0.2 mg of TiO_2. This is about 120 times less than the amount of TiO_2 in the suspension in Fig. 5 (trace d) leading to Methyl Orange photodiscoloration in the same volume (50 ml).

3.4. X-ray diffraction measurements

The parylene/TiO_2 films were examined by X-ray diffraction to find out if the crystallinity of the TiO_2 Degussa P25 powders used was affected by the preparation method. The results indicated that this was not the case since the presence of the anatase phase and rutile phase was found in the same ratio as in the TiO_2 Degussa P25 powders.

3.5. X-ray photoelectron spectroscopy of parylene/TiO_2 films

The elements atomic concentration on the parylene surface as detected by XPS are: Na 1.01%; N 1.55%; O 9.04%; Ca

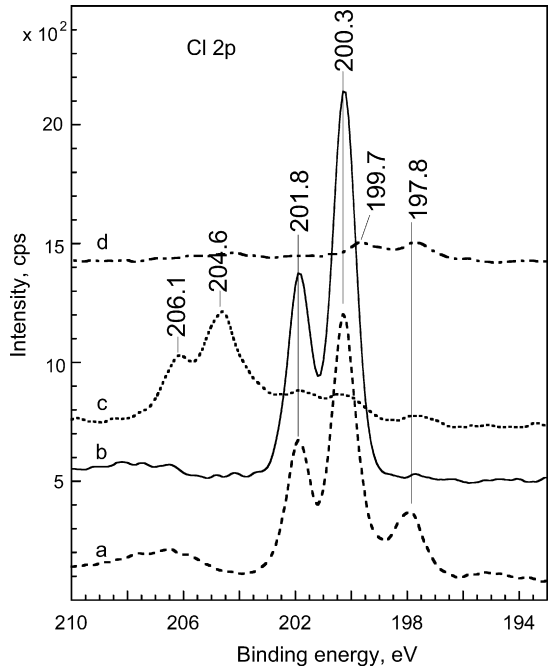

Fig. 10. Evolution of the Cl 2p XPS signals for: (a) parylene film alone, (b) parylene/TiO_2 at time zero, (c) parylene/TiO_2 after 3 h Suntest irradiation and (d) parylene/TiO_2 after 6 h Suntest irradiation during the photodiscoloration of Methyl Orange (0.01 mM).

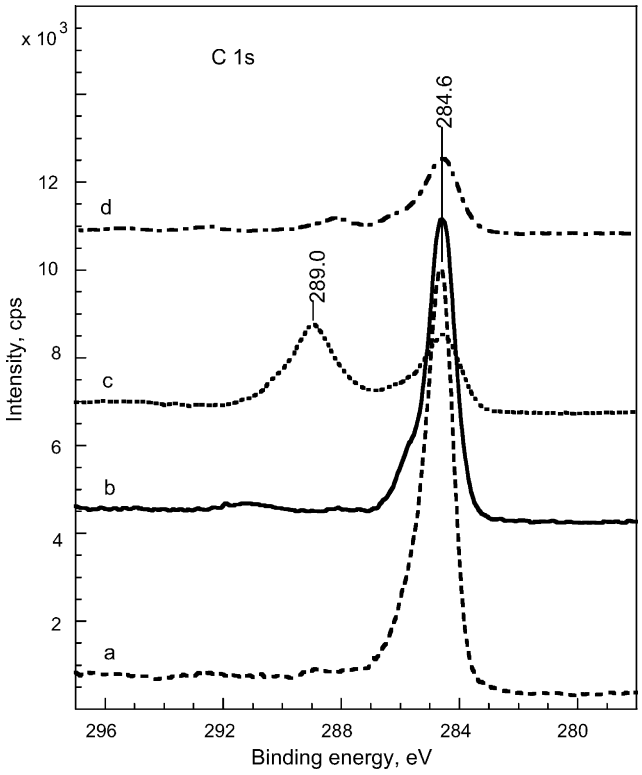

Fig. 11. Evolution of the C 1s XPS signals for: (a) parylene film alone, (b) parylene/TiO_2 at time zero, (c) parylene/TiO_2 after 3 h Suntest irradiation and (d) parylene/TiO_2 after 6 h Suntest irradiation during the photodiscoloration of Methyl Orange (0.01 mM).

0.42%; C 82.64%; Cl 4.54% and Si 0.81%. Parylene films alone show two components for the Cl 2p doublet with Cl $2p_{3/2}$ line positions at 200.3 and 197.8 eV (Fig. 10). These two components are the C–Cl and Cl^- types of chlorine, respectively (Fig. 10, trace a). Fig. 10 (trace b) shows the very strong signal of one type of the doublet Cl 2p line at 200.3 eV after the TiO_2 loading on parylene-C at time zero due to the C–Cl surface group. Fig. 10 (traces c and d) shows that during the dye discoloration, the Cl 2p signal shifts significantly on the catalyst surface after 3 and 6 h.

Parylene film alone also shows a major C 1s line at 284.6 eV due to the presence of aromatic CH– groups (Fig. 11). Fig. 11 shows no shift in the position of the C 1s line in traces (a and b). But after 3 h reaction the formation of intermediate carboxylates and carbonates are seen at 289.0 eV. These intermediates decompose after 6 h reaction not leaving C-intermediate residues on the parylene/TiO_2 surface.

After 3 h reaction the Cl 2p component is shifted to higher BE of 204.6 eV (Fig. 10, trace c) together with C 1s component at 289 eV (Fig. 11, trace c). Both lines are shifted nearly the same value of 4.3–4.4 eV indicating that they belong to the same surface species. These shifted bands are most probably generated by not fully detached pieces of parylene film showing very strong charging effect [23]. After 6h of reaction both of these pieces are completely removed from catalyst surface (see Fig. 10, trace d and Fig. 11, trace d). It is also interesting to note that after 6h of reaction there is almost no visible signal of the Cl-line, which indicates the parylene is not present at the interface in its original form. There is a small intensity Cl 2p line at 197.8 eV (Fig. 10, trace d) indicating the presence of Cl^-

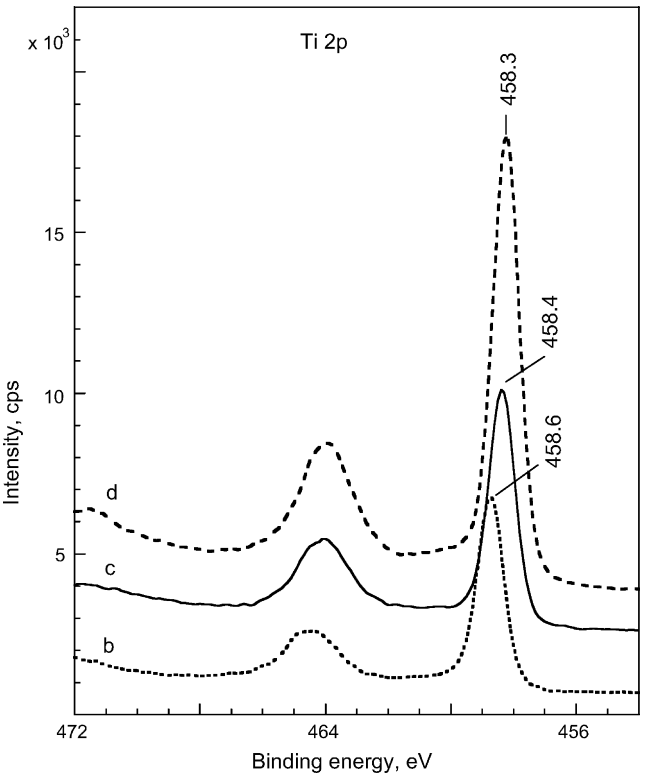

Fig. 12. Evolution of the Ti 2p XPS signals of (b) parylene/TiO_2 at time zero, (c) parylene/TiO_2 after 3 h Suntest irradiation and (d) parylene/TiO_2 after 6 h Suntest irradiation during the photodiscoloration of Methyl Orange (0.01 mM).

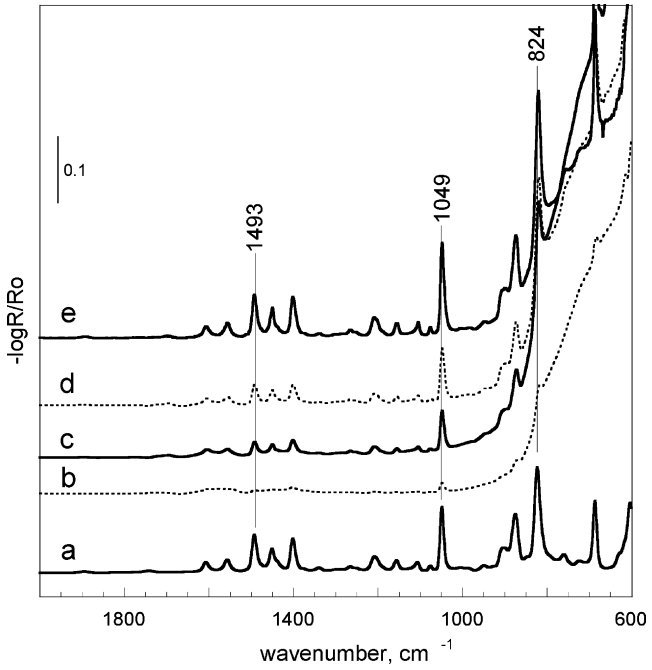

Fig. 13. Fourier transform infrared spectroscopy of: (a) parylene film alone, (b) parylene/TiO_2 at time zero, (c) parylene/TiO_2 after 1 h Suntest irradiation, (d) parylene/TiO_2 after 3 h Suntest and (e) after 6 h Suntest irradiation during the photodiscoloration of Methyl Orange (0.01 mM).

species. This points to a very dense loading of TiO_2 on the parylene film surface.

Fig. 12 (trace b) shows the strong signal of Ti $2p_{3/2}$ at 458.5 eV due to the TiO_2 particles deposited on the parylene-C surface. Fig. 12 (traces c and d) shows that after 3 and 6 h as the photodiscoloration of Methyl Orange progresses, the 458.5 eV line signal increase significantly. This means that after 3 and 6 h reaction, the parylene-C layer surrounding the TiO_2 particles is cracked and detaches from the TiO_2 particles and that the TiO_2 particles at time zero were encapsulated by parylene-C. The Ti 2p line is shifted from 458.6 to 458.3 eV towards a lower BE by 0.3 eV. This indicates a partial reduction of TiO_2 that acts as an oxidant since the shift towards lower energies reflects a lower oxidation state of Ti in TiO_2. The state of oxidation of Ti is therefore moving from 4 at zero reaction time to about 3.8 after 6 h reaction. The process associated with this shift is

$$TiO_2 + C \rightarrow TiO_{2-x} + C_{oxid} \quad (9)$$

and leads to the formation of carbonates and carboxylates as seen in Fig. 11 (trace c) at 289.0 eV during the dye photodiscoloration process.

The N 1s line at 399.5 eV was also found on the parylene/TiO_2 films with similar intensity, at different discoloration times of Methyl Orange. This lends support to the conclusion that there is no surface accumulation of Methyl Orange decomposition products during the photodiscoloration process. A broad O 1s line at 532.0 eV was detected indicating the presence of surface OH groups and several other minor oxygenated residues on the surface of parylene/TiO_2.

3.6. Infrared spectroscopy studies

The recorded attenuated total infrared reflection spectra ATIR of the parylene film alone and parylene loaded with TiO_2 after different reaction times are presented in Fig. 13. TiO_2 has a strong absorbance bands at 573 cm^{-1} with shoulder at 760 cm^{-1}, which appears in the recorded spectra in form of a strong increase of absorbance level below 800 cm^{-1}. The spectra of parylene loaded with TiO_2 and after different reaction times are almost exactly the same as the spectrum of parylene alone in Fig. 13. There is no clear presence of new absorbance bands indicating the formation of significant amount of intermediates at the catalyst surface or significant changes in the surface composition of parylene-C. The only clearly observed change after the decomposition reaction of Methyl Orange is the increase of the intensity of absorbance bands of parylene without decreasing absorbance $<$800 cm^{-1}. This indicates that TiO_2 particles are strongly bonded to the parylene film but undergo some modification during the discoloration of Methyl Orange. This was shown in a detailed way by the XPS data above in Section 3.5.

4. Conclusions

This study reports a novel innovative polymer film and the loading method for TiO_2. This functional material is shown to be useful as a photocatalyst in the discoloration of azo dyes. The parylene/TiO_2 characterization was carried out by TEM, X-ray diffraction and elemental analysis. The changes in the parylene/TiO_2 film during the photodiscoloration process have been followed by X-ray photoelectron spectroscopy and Fourier transform infrared spectroscopy.

Acknowledgement

We wish to thank the COST Action 540 PHONASUM ''Photocatalytic technologies and novel nano-surface materials, critical issues'' for the financial support of this study.

References

[1] Th. Oppenlaender, Photochemical Purification of Water and Air, Wiley-VCH Verlag, Weinheim, Germany, 2003.
[2] A. Mills, S. Lee, J. Photochem. Photobiol. A 152 (2002) 233–249.
[3] A. Fujishima, K. Hashimoto, W. Watanabe, Photocatalysis, Fundamental and Applications, Bkc Inc., Tokyo, Japan, 1999.
[4] J. Winkler, Titanium Oxide, Vincents Verlag, Hannover, 2003.
[5] J. Fernandez, J. Bandara, A. Lopez, Ph. Buffat, J. Kiwi, Langmuir 15 (1999) 185–192.
[6] M. Dhananjeyan, J. Kiwi, P. Albers, O. Enea, Helv. Chim. Acta 84 (2001) 3433–3445.
[7] M. Dhananjeyan, J. Mielczarski, K. Thampi, Ph. Buffat, M. Bensimon, A. Kulik, E. Mielczarski, J. Kiwi, J. Phys. Chem. B 105 (2001) 12046–12055.
[8] T. Yuranova, O. Enea, E. Mielczarski, J. Mielczarski, P. Albers, J. Kiwi, Appl. Catal. B 49 (2004) 39–50.
[9] A. Bozzi, T. Yuranova, J. Kiwi, J. Photochem. Photobiol. A 172 (2005) 27–34.
[10] T. Yuranova, R. Mosteo, J. Bandara, D. Laub, J. Kiwi, J. Mol. Catal. A 244 (2006) 160–167.

[11] Yu. Zhiyong, E. Mielczarski, J.A. Mielczarski, D. Laub, L. Kiwi-Minsker, A. Renken, J. Kiwi, J. Mol. Catal. A 260 (2006) 227–234.
[12] C. Morrison, J. Bandara, J. Kiwi, J. Adv. Oxid. Technol. 1 (1996) 160–169.
[13] J. Kiwi, C. Lizama, J. Freer, D. Mansilla, J. Photochem. Photobiol. A 151 (2002) 213–219.
[14] A. Shirley, Phys. Rev. A 179 (B5) (1979) 4709–4716.
[15] D. Briggs, M. Shea, Practical Surface Analysis, second ed., Auger and X-ray Photoelectron Spectroscopy, vol. 1, John Wiley, Chichester, UK, 1990
[16] J.N. Harrick, Internal Reflection Spectroscopy, Harrick Scientific Co., Ossining, New York, USA, 1989.
[17] Disperse Metal-oxides, Degussa AG, 6342 Baar 2, Switzerland, 1997.
[18] J. Bandara, J. Mielczarski, J. Kiwi, Langmuir 15 (1999) 7680–7686.
[19] K. Vinodgopal, P. Kamat, J. Photochemistry Photobiol. A 83 (1994) 141–148.
[20] J. Bandara, J. Kiwi, N. J. Chem. 23 (1999) 717–724.
[21] L. Lucarelli, V. Nadtochenko, J. Kiwi, Langmuir 16 (2000) 1102–1108.
[22] J. Kiwi, M. Gràtzel, J. Mol. Catal. 39 (1987) 63–70.
[23] C. Wagner, W. Riggs, I. Davis, J. Moulder, G. Muilenberg (Eds.), Handbook of X-ray Photoelectron Spectroscopy, Perkin Elmer Corp., Eden-Prairie, MN 55344, USA, 1989.